Materials Advances

Accepted Manuscript

This article can be cited before page numbers have been issued, to do this please use: V. Nutalapati, P. Palanisamy, M. Anandan, S. Sasi, A. Bora, R. P. Reji, C. B. Sarath Kumar, Y. Kawazoe, K. Kommineni, S. Velappa Jayaraman and Y. Sivalingam, *Mater. Adv.*, 2025, DOI: 10.1039/D4MA01228C.

View Article Online
DOI: 10.1039/D4MA01228C

Orthogonal effect on Pyrene-Porphyrin conjugates towards the detection of Volatile Organic Compounds under UV and Visible light illumination through Surface Photovoltage

Prasanth Palanisamy[a], Mageshwari Anandan[a], Sheethal Sasi[b], Arbacheena Bora[b], Sarath Kumar Chedharla Balaji[c], Rence P Reji[c], Yoshiyuki Kawazoe[d,e], Kommineni Kalyani[f], Surya Velappa Jayaraman[c,d*], Yuvaraj Sivalingam[b,e] and Venkatramaiah Nutalapati[a*]

[a] *Functional Materials Laboratory, Department of Chemistry, Faculty of Engineering and Technology, SRM Institute of Science and Technology, Kattankulathur 603203, India.*

[b] *Laboratory of Sensors, Energy and Electronic Devices (Lab SEED), Department of Physics and Nanotechnology, SRM Institute of Science and Technology, Kattankulathur 603203 Tamil Nadu, India.*

[c] *Novel, Advanced, and Applied Materials (NAAM) Laboratory, Department of Physics and Nanotechnology, SRM Institute of Science and Technology, Kattankulathur 603203 Tamil Nadu, India.*

[d] *New Industry Creation Hatchery Centre (NICHe), Tohoku University, Aoba-ku, Sendai 980-8579, Miyagi, Japan.*

[e] *Computer, Electrical and Mathematical Sciences and Engineering Division (CEMSE), King Abdullah University of Science and Technology (KAUST), Thuwal 23955-6900, Kingdom of Saudi Arabia.*

[f] *Department of Chemistry, RVR&JC College of Engineering, Guntur, Andhra Pradesh 522019, India*

To whom correspondence should be addressed
Dr. Venkatramaiah Nutalapati, E-mail: nvenkat83@gmail.com/venkatrv1@srmist.edu.in
Dr. Surya Velappa Jayaraman, Email: suryaj@srmist.edu.in.

View Article Online
DOI: 10.1039/D4MA01228C

Abstract

In this work, we have developed two modular compounds encompassed with pyrene at *meso* position of the freebase porphyrin (H_2PyP) and its complex with Zn (ZnPyP). Both compounds exhibited to show a unique energy transfer process due to the orthogonal pyrene units and reveal that appreciable electronic interactions exist between peripheral units to the porphyrin π-system and behave like strong donor materials in solid-state thin films. Detailed photophysical and excited state gas phase interactions were modulated through surface photovoltage using Scanning Kelvin Probe (SKP) technique and explored towards detection of different volatile organic compounds (VOCs) (Ethanol, Acetone, 1-Hexanol, Triethylamine, Nonanal, and Acetonitrile) in dark, UV and visible light illuminations. H_2PyP and ZnPyP show *n-type* behaviour with high selectivity towards 1-hexanol under UV light illumination while under visible light illumination, ZnPyP exhibits *n-type* and H_2PyP show *p-type* behaviour. The response and recovery studies demonstrate that H_2PyP and ZnPyP show unprecedented selectivity towards 1-hexanol by altering it *p* and *n* type behaviour. H_2PyP exhibits a high photovoltage response of 93% for an exposure of 17 s with a recovery rate of 23% in 5 s, while ZnPyP show 97% in 2 s with a recovery rate of 55% in 116 s under UV light. The unique response of H_2PyP and ZnPyP to 1-hexanol could be attributed to donor-donor interaction and intermolecular hydrogen bonding at central core and variations in the energy transfer process. Further, density functional theory study reveals that binding interactions of H_2PyP and ZnPyP with VOCs show greater affinity for alcohol vapours in comparison to other compounds.

Keywords: Porphyrins; Pyrene; Volatile Organic Compounds (VOCs); Scanning Kelvin Probe (SKP); Gas Adsorption

1. Introduction

View Article Online
DOI: 10.1039/D4MA01228C

Volatile organic compounds (VOCs) are abundant in the environment and present substantial risks to human health and safety.[1] The identification of VOCs is essential for a wide range of purposes, such as monitoring the environment, controlling industrial processes, and ensuring national security.[2-5] Among the various toxic VOCs, 1-hexanol and nonanal are used as biomarkers in fishes and monitoring the emission of these VOCs evident the freshness of the fish.[6,7] Conventional techniques for detecting VOCs typically require sophisticated equipment and may have limitations in terms of sensitivity or specificity.[8] The scanning Kelvin probe (SKP) technique is a highly sensitive and non-invasive method for detecting VOCs.[9] It measures the variations in the contact potential difference (CPD) between a reference probe and a sample surface, making it a powerful tool for VOC sensing. This method is especially beneficial for detecting VOCs due to its non-invasive approach and provide precise measurements in real-time without requiring direct contact with the sample. Hence, it minimizes the risk of contamination and interference.[10] Incorporation of SKP with cutting-edge materials, such as organic semiconductors and hybrid systems, has increased its efficiency in detecting VOCs. Utilization of materials possessing customized electronic characteristics and elevated surface reactivity can enhance the sensitivity and selectivity of the SKP technique. It can detect a broad spectrum of VOCs at low levels and in different environmental circumstances.[11]

Porphyrins play a vital role in augmenting the capabilities of SKP techniques for detecting VOCs. Due to their distinctive chemical and electronic properties, they are exceptionally efficient as a sensor material.[12] It possess a substantial surface area and exhibit significant reactivity as a result of their conjugated ring systems.[13] The high surface area increases their capacity to adsorb VOCs, resulting in more noticeable alterations in the chemiluminescence peak detected by SKP as/or *n-type* and *p-type* behaviour.[14] The interaction between porphyrins and VOCs can result in detectable changes in charge transfer processes, enabling the identification of even very low concentrations of VOCs.[15] By modifying the metal centres or substituent groups, one can precisely adjust the electronic characteristics of porphyrins. The ability to adjust and control the properties of porphyrin-based sensors enables the creation of sensors that have specific attractions to various VOCs.[16] By careful choice of porphyrin derivatives, sensors can be enhanced to detect specific VOCs, enhancing selectivity and minimizing interference from other substances.[17] The orientation of substituents at meso position with orthogonal approach exhibits an efficient intra molecular electron/energy transfer process through favourable for extended π–π electronic interactions for effective long lived ion

View Article Online
DOI: 10.1039/D4MA01228C

pair states. These configurations have the potential to improve singlet energy transfer, which is crucial for solar energy conversion and photodynamic treatment applications.[18] Induction of rigid fused aromatic structures like pyrene at meso position of porphyrin molecules improves the π-π stacking interactions in these systems and increases the mobility of charge carriers due to the orthogonal effect.[19]

By incorporating meso-substituted porphyrins and metalloporphyrin into SKP-based sensors, becomes excellent technique to detect volatile organic compounds (VOCs) in real-time with a high level of sensitivity.[20] Extended conjugation offers a huge opportunity to construct organic semiconductors based on the D-D framework because of the pervasiveness of the charge transfer process in D-D molecules. The behaviour of naphthalene attached DPP molecules functionalized with ZnO nanostructures synthesised at different pHs (pH 9 and 11) in terms of gas adsorption has been shown by Marappan *et al.* to exhibit a greater photo response towards 1-hexanol at pH 11.[21] Our group has recent reported on the polymorphism-driven gas adsorption on the naphthalic imide decorated phenothiazine unit surface shows that preferential photo response toward VOCs is induced by surface morphology and interaction sites.[22] Elakia *et al.* investigated the gas sensing properties of pyrene molecules with −COOH functionality coated on multi-walled carbon nanotubes. The study reports that pyrene coupled to −COOH exhibits powerful intermolecular H-bonding mediated by D−A contact, resulting in good selectivity for triethylamine with favourable response and recovery.[23] As a biomarker for liver diseases, Sivalingam *et al.* demonstrated how gas adsorption impacts the surface of a phthalocyanine-coated TiO_2 thin film. The VOC that patients with liver illnesses exhale through their breath is triethylamine, and the functionalized thin film demonstrated improved sensitivity and selectivity for triethylamine detection.[24] Reji *et al.*, on the other hand, published VOC adsorption tests on Fe(II)phthalocyanine and metal-free samples, which demonstrated solid-state J-aggregation. Fe(II)phthalocyanine displays a selective photoresponse to nonanal and 1-hexanol under dark and visible light illumination, respectively, in contrast to the metal-free phthalocyanine.[25] By using DFT, Wang *et al.* examined the ground-state molecular structure, electron distribution, and UV spectra features of octaethyl porphyrins with various central metals (M-OEP, M=Ni, V, O, Cu, and Co). The results demonstrate that there was a good agreement between the experimental value and the computational structure parameters of metalloporphyrins.[26] Gawas *et al.* reported the substituent effect on stimuli-responsive donor-acceptor framework-Based 2-thiohydantoins for nonanal vapour monitoring. The structure-function link examined in this work may offer important insights for the creation of highly

View Article Online
DOI: 10.1039/D4MA01228C

effective gas sensor and also showed the effect of extended π-Conjugation on 2-thiohydantoins to a strictly defined volatile organic compound detection by surface photovoltaics.[27,28] Sasi *et al.* developed a surface of boron-doped diamond (BDD) functionalized with 5-(4-carboxyphenyl) triphenyl porphyrins, and gas adsorption was investigated at room temperature. Using SKP system, the surface potential distribution caused by the adsorption of VOCs under visible light illumination conditions was examined following the structural and morphological characterisations of the porphyrin-functionalized BDD surface and the bare BDD surface. Under visible light porphyrin functionalized BDD thin film showed selective response towards triethylamine.[29] Marappan *et al.* investigated vertically grown ZnO NRs functionalized with TPA derivatives capacity for VOC sensing. Under dark conditions, the functionalized ZnO NRs exhibit superior gas sensitivity towards nonanal, as demonstrated by the SKP experiments. It shows excellent adsorption towards nonanal under light illumination.[30] Based on the literature report our synthesised organic material work was suitable for gas adsorption studies to find the new novel of the structural reactivity and provide new avenue to have selective detection towards VOCs.

In this report, we have described the synthesis and photophysical properties of pyrene tethered meso substitute freebase porphyrin and its Zn(II)complex to ascertain the role of orthogonal effect of molecular ensembles on the gas adsorption behaviour with different VOCs through the change in the surface photovoltages. The change in the work function of the material by the adsorption of VOCs on the sample surface due to physisorption or chemisorption was monitored under dark, UV and visible light illumination. Under UV and visible light illumination, the highest photo voltage response was exhibited by 1- hexanol followed by nonanal. By modifying the D-D (Donor-Donor) design with different donors that overlap with higher electron densities, selectivity to VOCs is achieved, as well as quick recovery. The detailed mechanistic investigation on photoresponse behaviour is further analysed in light with binding behaviour with density functional theory (DFT).

2. Materials and methods

All the A.R grade chemicals and solvents were procured from Sigma Aldrich and Avra Chemicals Ltd, India, used directly without additional purification. Fourier-transform infrared (FT-IR) spectra were recorded using Shimadzu IR Tracer-100 under KBr mode. NMR (^{1}H and ^{13}C) spectra were measured at 300 MHz with TMS as the internal reference. ESI-MS analysis was carried out in LC-MS 2020 system equipped with an LC10ADVP binary pump (Shimadzu, Japan). Agilent Cary 60 UV-Vis spectrometer was used to record the absorption spectra in both

View Article Online
DOI: 10.1039/D4MA01228C

thin films and solutions. Steady state fluorescence spectra of thin films were measured in FLS 1000 photoluminescence spectrometer. Contact potential difference (CPD) measurements were made using a surface photovoltage module using a 2 mm vibrational gold tip operating at 78.3 Hz in the Scanning Kelvin Probe System (SKP) (SKP5050, KP Technology Ltd., UK). HR-TEM images were obtained using JEOL 2100 transmission electron microscope. High-resolution scanning electron microscope (HR-SEM) images were obtained from a Thermo Scientific Apreo S spectrometer. Ground state geometry optimization was carried out in Gaussian16 software with a basis set of 6-311++G (d,p)/LANL2DZ with hybrid functions in B3LYP and visualization was made with Gauss View 5.2 suit software.

2.1. Synthesis

2.1.1. Synthesis of *meso*-5,10,15,20-tetrakis(pyren-1-yl)porphyrin (H_2PyP)

In a 500 mL round base flask, distilled propionic acid (200 mL) and pyrrole (0.583 mL, 8.6 mmol) was taken. To this pyrene-1-carbaldehyde (2g, 8.6 mmol) is added and the reaction mixture was kept for refluxing at 150 °C under air condition. The progress of the reaction was monitored by TLC Chromatography. The reaction mixture was cooled to room temperature and kept in the refrigerator for overnight. The obtained black color precipitate was filtered off under vacuum and washed thoroughly with water and methanol. Finally, silica gel column was employed to purify the product using Hexane: chloroform as eluent (20:80, v/v%). Yield. 2.3%. ^{1}H NMR (300 MHz, $CDCl_3$) (ppm): δ 8.86-8.75 (m, 3H), δ 8.46-8.42 (m, 10H), δ 8.34-8.25 (m, 12H), δ 8.07-7.99 (m,10H), δ 7.74-7.69 (m,4H), δ 7.64-7.60 (m,2H) δ 7.58-7.46 (m,3H) and δ -1.96 (s, 2H, N-H). ^{13}C NMR (75 MHz) δ (ppm): 131.71, 131.47, 130.79, 128.06, 127.64, 126.29, 125.32, 125.02, 122.81 and 122.78. ESI-MS: calcd for $C_{84}H_{46}N_4$ (m/z): 1110.3722; found: 1134.2000 $[M+Na]^+$.

2.1.2 Synthesis of *meso*-5,10,15,20-tetrakis(pyren-1-yl)porphyrinato Zinc(II) (ZnPyP)

Freebase porphyrin (H_2PyP) (70 mg, 0.062 mmol) was dissolved in THF (5 mL) and the solution was purged with nitrogen for 10 min. A solution of $Zn(OAc)_2$ (20.7 mg, 0.094 mmol) in MeOH (3 mL) was added to the H_2PyP solution, and the reaction mixture was stirred overnight. The solvent was removed under vacuum conditions and purified through silica gel column gives brown solid. Yield. (65 mg, 87%). ^{1}H NMR (300 MHz, $CDCl_3$) (ppm): δ 8.89-8.76 (m, 3H), δ 8.51-8.45 (m, 7H), δ 8.35-8.33 (m, 7H), δ 8.29-8.24 (m, 5H), δ 8.07-8.00 (m,5H), δ 7.99 (s,1H), δ 7.75-7.67 (m,6H) and δ 7.62-7.45 (m,3H) ^{13}C NMR (75 MHz, $CDCl_3$) (ppm): δ 151.31, 132.63, 132.52, 132.47, 131.75, 131.30, 130.82, 127.90, 127.66, 126.21,

View Article Online
DOI: 10.1039/D4MA01228C

125.47, 125.47, 125.19, 124.65, and 122.661. ESI-MS: calcd for $C_{84}H_{46}N_4$ (m/z): 1174.3650; found: 1176.2500 $[M+2H]^+$.

2.2 Scanning Kelvin Probe measurements for Gas adsorption studies

To study the gas adsorption properties of the samples, SKP measurements were carried out. Fluorine doped tin oxide (FTO) coated glass substrates (~15 Ω) of dimension 2x2 cm^2 were washed with soap solution, distilled water, acetone, and ethanol in an ultra-sonicated bath for 30 minutes at 55 ºC after which it was spin coated with H_2PyP and ZnPyP. After the coated films had dried for 4h at room temperature, gas adsorption studies performed, under the SKP module. To measure the change in the photovoltage of H_2PyP and ZnPyP upon exposure to different VOCs under dark and light conditions, the measurements were performed in a closed chamber at ambient temperature (~25 ºC). In order to investigate the effect of light impact on the gas adsorption behaviour, two different light sources quartz tungsten halogen (QTH) lamp as visible light source and long UV light (365 nm) was used as irradiation sources. Initially, the measurements were performed under air medium as a reference. Then, different VOCs with varied vapour pressures like acetone, ethanol, 1-hexanol, acetonitrile, nonanal, and triethylamine were chosen to ascertain its donor and acceptor nature. Concentration based studies were not done in the SKP chamber. Instead, constant amount (~20 mL) of each VOC was exposed and allowed to vapourize inside the chamber at 25 ºC for a constant time (~10 minutes) and then the measurements were performed. The volatility of the measurements was maintained by normalizing the measurements with corresponding vapour pressures of each VOCs. The results were divided by the saturated vapour pressure (SVP) of each VOC at 25 ºC. The SVP was calculated from Antoine's equation (1) at 25 ºC.

$$\log (\mathrm{Pi}) = A - \frac{B}{C+T} \qquad (1)$$

where A, B and C are Antoine's parameters, Pi is the vapour pressure of VOC and T is the temperature (25 ºC).

3. Results and Discussions

Freebase porphyrin (H_2PyP) having four pyrene units at meso position was synthesized by Adler's method through reflux condensation reaction between pyrrole and 1-Pyrenecarboxaldehyde in propionic acid medium for 2h (Scheme 1). Column chromatography was used to isolate and purify the target compound and characterized. Further, metalation of H_2PyP with $Zn(OAc)_2$ was carried out in THF and methanol to obtain ZnPyP with 80% yield.[31] The FT-IR spectrum of H_2PyP reveals distinctive vibrational peak at 3307.45 cm^{-1}

View Article Online
DOI: 10.1039/D4MA01228C

corresponding to N-H stretching, a peak at 1583 cm^{-1} indicating C=C bonds, another peak at 1453 cm^{-1} representing C=N bonds, a band at 1343 cm^{-1} for C-N bonds, a signal at 1052 cm^{-1} associated with aromatic structures and a peak at 961 cm-1 attributed to aromatic C-H bonds. Upon metalation, C=C band shifts to 1586 cm^{-1}, while the C=N and C-N bands shift to 1334 cm^{-1} and 1250 cm^{-1}, respectively (Fig. S1, ESI†). The ^1H NMR spectrum of H_2PyP showed a singlet signal due to -NH protons at highly shielded region at δ -1.96 ppm, and the aromatic β-pyrrole and meso-pyrenyl protons of H_2PyP resonate in the aromatic region at δ 8.86–7.46 ppm (Figs. S2-S3, ESI†). For ZnPyP, the singlet signals attributed to the -NH protons disappeared, while the aromatic region remained between δ 8.89-7.45 ppm (Figs. S4-S5, ESI†). ESI-MS spectra of H_2PyP and ZnPyP showed molecular ion peaks at m/z 1134.2000 $[M+Na]^+$, and 1176.2500 $[M+2H]^+$ respectively, which corroborate the final desired compounds (Figs. S6-S7, ESI†).

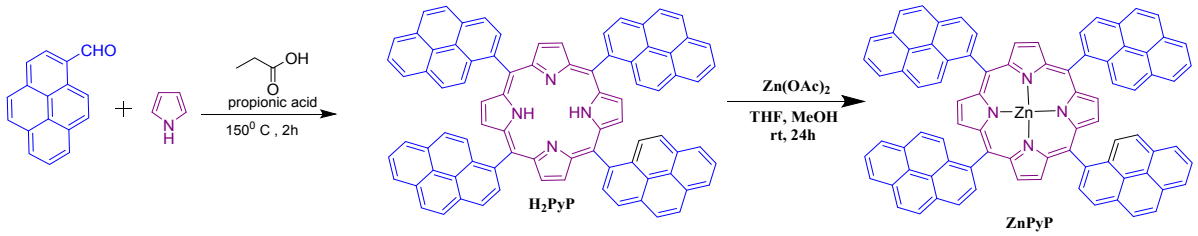

Scheme1. Synthesis routes for H_2PyP with ZnPyP.

Fig. 1a shows the absorption spectra of H_2PyP and ZnPyP in thin films coated on the quartz substrate. H_2PyP T.F showed a broad Soret band absorption at 450 nm along with four Q-band patterns in the region of 520-660 nm. In addition, we have observed a vibronic absorption band at 235 nm ($S_0 \rightarrow S_4$), 264 nm ($S_0 \rightarrow S_3$) and broad absorption at 320-330 nm region corresponds to $S_0 \rightarrow S_2$ transitions of pyrene.[32,33] The Soret band show strong red shifted absorption in comparison with H_2TPP due to extended conjugation of pyrene. ZnPyP T.F shows Soret band at 450 nm along with Q bands at 566 and 633 nm. The four Q-band patterns changed to two band pattern confirms the metalation at the central core. The absorption of pyrene in ZnPyP T.F show much broader with red shifted in comparison with H_2PyP T.F. The absorption spectra in thin films are found to be broader and red shifted than in the solution by ~5-10 nm shifts due its strong molecular arrangement (Fig. S8, ESI†). Pyrene shows different emission behaviour as monomer emission centred at 383 nm and excimer emission at 470 nm. Free base porphyrin (H_2TPP) shows two band emissions at 652 and 715 nm originating from $S_1 \rightarrow S_0$ transition. Steady state emission spectra of H_2PyP T.F at different excitation

View Article Online
DOI: 10.1039/D4MA01228C

wavelengths were carried out to ascertain the emission behaviour due to different mode of conjugation. On excitation of H_2PyP T.F at λ_{ex}= 330 nm, we have observed three different broad emission bands centred at 438, 452 and 469 nm along with an intense broad emission at 650-750 nm region which is attributed due to $S_1 \rightarrow S_0$ emission of the Soret band. The emission peak at 469 nm corresponds to the emission features of the excimer emission. The observed red shift in comparison to pristine compounds indicates the increase in the conjugation of pyrene due to orthogonal orientation as similar to the absorption spectra. The spectral overlap of pyrene emission and Soret band absorption indicates that intramolecular energy transfer from peripheral pyrene to H_2PyP T.F. A similar observation was made for H_2PyP T.F dissolved in chloroform solution (Fig. S8, ESI†). Fig. 1b shows the emission spectra of ZnPyP T.F at different excitation wavelengths. Upon excitation at 330 nm, the monomer emission is predominant than the excimer emission and the energy transfer process is more prominent for H_2PyP T.F than ZnPyP T.F. It may arise due to orientation of pyrene units at meso position and variations in the planarity (Fig. S9, ESI†).

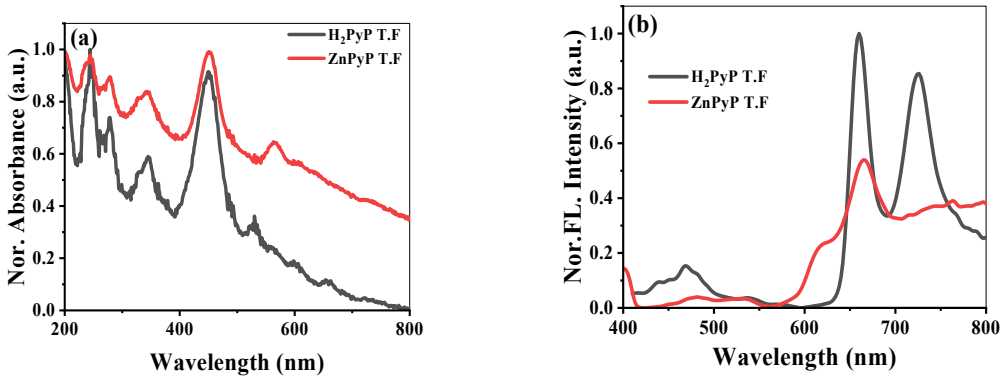

Fig. 1. Absorption spectra of H_2PyP and ZnPyP coated on the quartz substrate. (b) Emission spectra of H_2PyP and ZnPyP thin films upon excitation at λ_{ex} = 330 nm.

Surface topology, microstructure and roughness of thin films were analysed through HR-SEM, and HR-TEM as shown in Fig. 2. Thin films were developed by dissolving both the compounds in a chloroform solvent with a concentration of 5 mg/mL at room temperature. The films are fabricated by spin coating and then annealing up to 100°C for 30 min for better self-assembly. The resulted films are homogenous with maximum surface coverage. The scanning electron microscopic (SEM) analysis is carried out to determine the self-assembly characteristics of the active layer. Due to large planar nature of porphyrin core along with pyrene units which tend to undergo aggregation behaviour and results in the formation of large spherical aggregates on

View Article Online
DOI: 10.1039/D4RA01228C

the surface (Fig. 2a). ZnPyP exhibited agglomerates with small spherical particles resembling nano-flowers (Fig. 2b).[34]

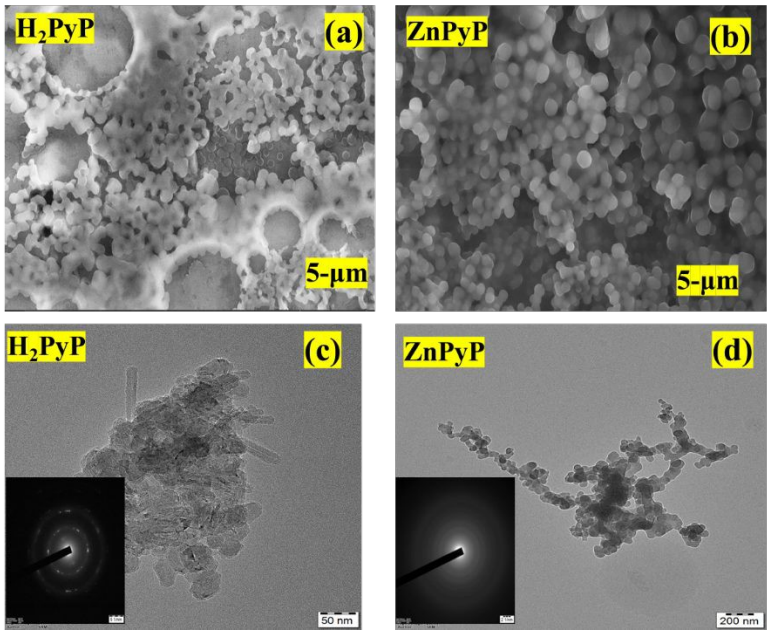

Fig. 2. HR-SEM images of (a) H_2PyP (b) ZnPyP; High-resolution transmittance electron microscopy images of H_2PyP (c) overall picture agglomerated, & inset SAED pattern of poly crystalline and ZnPyP (d) Zn particles obtained agglomerated carbon layer, inset image SAED pattern of amorphous.

The HR-TEM images of H_2PyP (Fig. 2c) show bright and images with crystalline behaviour indicated by SAED pattern. This behaviour is found to be decreased in ZnPyP (Fig. 2d). The inter-planar distances were measured to be 0.25 Å. The uniform distribution of thin film surface morphology suggests that the compounds self-assembled due to strong intermolecular interactions with energy transfer process and variation in the surface morphology tailored us to study the gas phase adsorption interactions with VOCs. To understand the gas adsorption phenomenon, SKP studies were performed to measures the change in the photovoltage of H_2PyP than ZnPyP upon exposure to different VOCs under UV and Visible light conditions. Scanning the surface facilitates the verification of the quality of the applied layer, ensuring consistent functionality, including uniform sensor response and electrical conductivity. The uniform CP value throughout the SKP map signifies that the surface exhibits relative homogeneity in its electronic properties, which is advantageous for specific materials, including thin films utilized in optoelectronics. Moreover, reproducible and consistent CP values across the surface validate the stability and accurate calibration of the SKP set up. 3D raster scanning of surface helps in understanding the homogeneity of the certain area of surface

View Article Online
DOI: 10.1039/D4MA01228C

upon VOC adsorption. Whereas, single point CPD measurements only gives information about a particular point above which the probe vibrates. A 2 mm diameter gold tip was used as a reference tip and the alteration in the CPD was recorded under dark and both sources of light. The vibrational frequency of the tip is 78.3 Hz. The gold tip is placed above the surface of the sample (Fig. 3a). An electrostatic force (F_ω) is felt when the gold tip and sample surface are close together F_ω is given by the following equation:[35]

$$F_\omega = \frac{-\partial C}{\partial V}\left(V_{off} - V_s\right)V_{ac}sin\omega t \text{---------(2)}$$

The CPD is estimated based on the surface potential (V_s) while the electrostatic force (F_ω) between the gold tip and the sample is negated. Utilising an external voltage (V_{off}) through a feedback loop, this surface potential is nullified. A standardised grade gold sample is used to scale the Au tip prior to each measurement. The interplay between the organic molecules and the gaseous environment is calculated based on the changing CPD values. According to the electron-donating or electron-accepting nature of the VOCs involved, the CPD of the samples was assessed with exposure to six different VOCs. All of the samples were initially compared to air medium. As a result of light illumination being exposed to the organic samples, photogenerated electrons are produced. As the measurements were not carried out by varying the VOC concentrations, the results were normalized using the SVP (equation 1) of each VOC at 25 °C to compare the volatility of the VOCs.

View Article Online
DOI: 10.1039/D4MA01228C

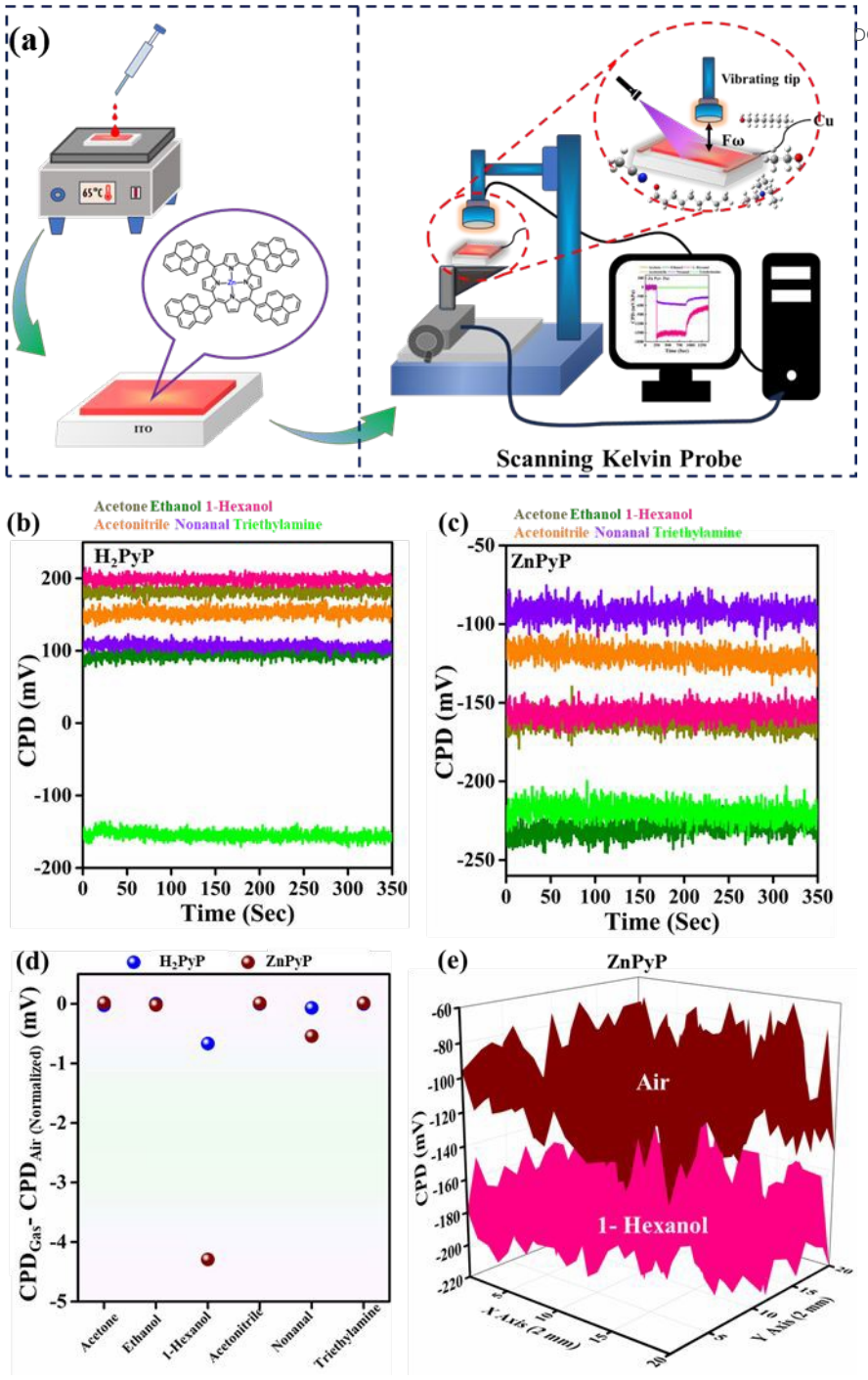

Fig. 3. (a) Schematic illustration of SKP device used in the present work. The time evolution of CPD signal under various VOCs exposure at dark for (b) H_2PyP and (c) ZnPyP (d) normalized CPD plots in VOCs with respect to air for the samples and (e) 3D raster scan image under ambient air and 1-hexanol for ZnPyP.

As shown in Fig. 3a, an SKP experimental setup was used to quantify changes in surface photovoltages in order to examine the gas adsorption characteristics of H_2PyP and ZnPyP. The

View Article Online
DOI: 10.1039/D4MA01228C

CPD values of H_2PyP and ZnPyP in VOCs under dark condition are given in Fig. 3b and 3c respectively, which gives the distinction between interactions of molecules to each VOC. Fig. 3d represents the normalized CPD measured for H_2PyP and ZnPyP molecules with respect to air under dark medium for different VOC atmospheres. These scatter plots clearly portray the selectivity of the molecules towards 1-hexanol vapours which is followed by the response of nonanal. From the raster scanned images of ZnPyP under air and 1-hexanol media, it is evident that the higher response aroused for ZnPyP in comparison with H_2PyP (Fig. 3e). Pyrene tetratopic ligands (PTL) functionalized multiwalled carbon nanotubes (MWCNTs) under light and illumination conditions upon exposure with triethylamine (TEA) vapours interact with acid base interactions through photo induced electron transfer process.[23] In the same case pyrene coated zinc oxide nanorod as showed good response to triethylamine.[36] In contrast, pyrene appended porphyrin derivatives show higher response through energy transfer process to 1-hexanol under dark and air conditions.

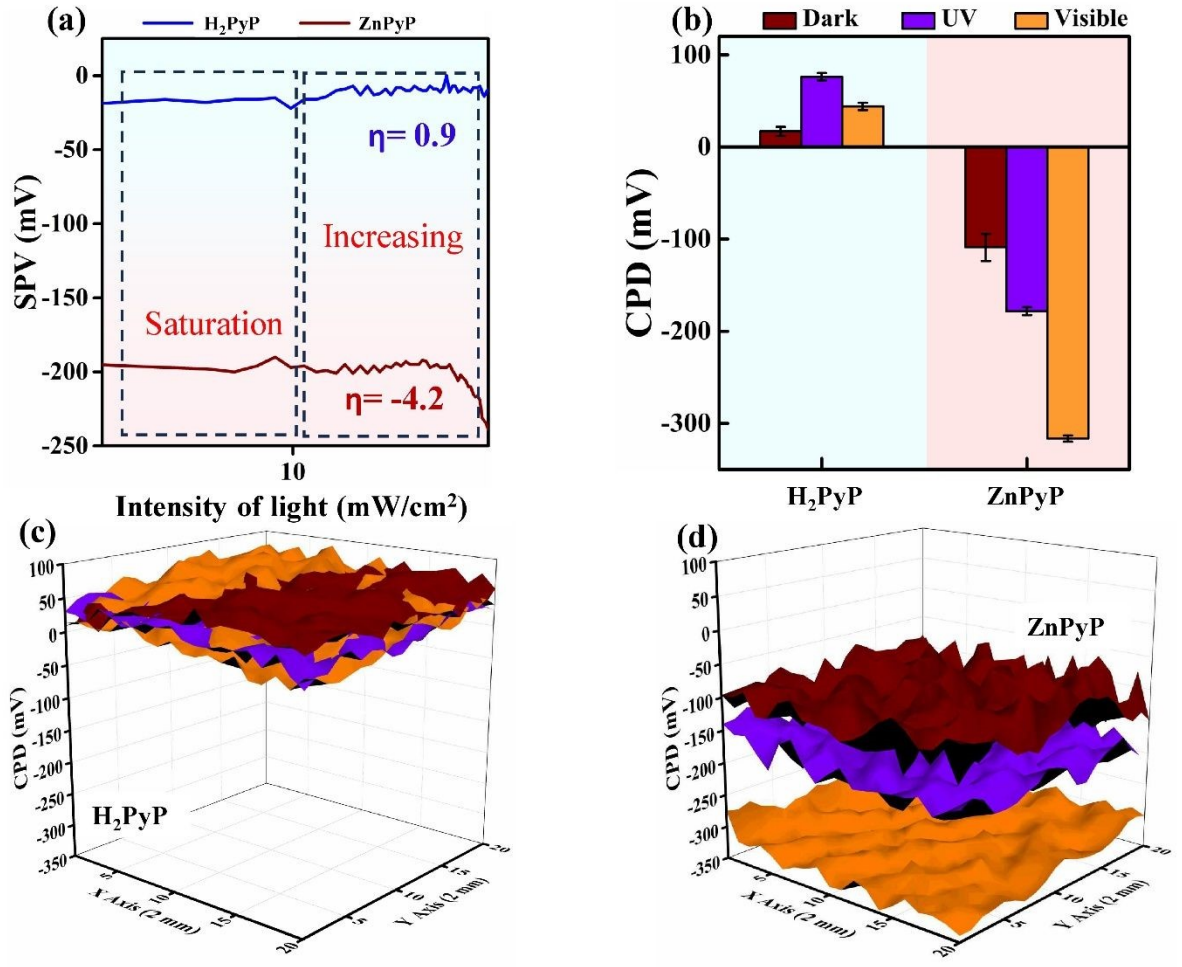

View Article Online
DOI: 10.1039/D4MA01228C

Fig. 4 (a) Surface photovoltage changes of H_2PyP and ZnPyP in air medium (b) CPD changes from dark to UV and visible light illumination in H_2PyP and ZnPyP. 3D raster scan images under dark, UV and visible light illumination in (c) H_2PyP and (d) ZnPyP under ambient air atmosphere.

Fig. 4a describes the surface photovoltage (SPV) of H_2PyP and ZnPyP. SPV does not show any significant change until a threshold value of ~12 mW/cm^2 is reached which arises due to insufficient concentration of photo generated charge carriers due to lower intensity of light not prominent enough to introduce the band bending effect. Once the threshold is crossed, SPV begins to increase in a linear pattern in ZnPyP molecule showing the highest altitude under air medium. Upon VOCs exposure, the highest slope is observed in 1-hexanol for both the compounds (Fig. S10, ESI†). The CPD values in dark medium for the gases under test are given in Table. 1.

Table.1. Change in the CPD values in dark medium for H_2PyP and ZnPyP under different VOCs exposure.

Molecular Substate	CPD values under dark medium (mV)					
	Acetone	Ethanol	1-Hexanol	Acetonitrile	Nonanal	Triethylamine
H_2PyP	58.37	113.84	25.20	20.56	89.71	-58.84
ZnPyP	-119.76	-93.91	-152.08	-132.95	-92.99	-138.51

The slope values obtained from the SPV plot is -1.5 mV/decade, -1.07 mV/decade, -2.21 mV/decade, -0.57 mV/decade, -1.95 mV/decade and -0.57 mV/decade for the H_2PyP and -0.11 mV/decade, -0.17 mV/decade, -1.11 mV/decade, -0.49 mV/decade, -0.995 mV/decade, -0.37 mV/decade for ZnPyP for acetone, ethanol, 1-hexanol, acetonitrile, nonanal, triethylamine respectively. An empirical formula was utilised to understand the direct proportionality relationship between the magnitude of surface photovoltage generated and the degree of brightness of the light which is as follows,[37,38]

$$SPV = \frac{\eta kT}{e} \ln (BI) \qquad \text{---------- (3)}$$

View Article Online
DOI: 10.1039/D4MA01228C

where I is the fluctuating light intensity, η and B are proportionality constants. To verify the proportionality constant which gives a measure of the defect state present in the nanostructure, the fitted data is considered. Greater the value of the slope, greater is the presence of defects in the structure. Upon exposure to 1-hexanol, we have observed the highest η value of -5.09 and -10.09 for H_2PyP and ZnPyP respectively. The η values of other VOCs are tabulated in (Table S1 and Fig. S8 ESI†) respectively. Fig. 4b represents the resultant CPD that arises when the organic samples are switched between dark and light condition, both UV and visible in ambient air. The CPD signal's noise value is addressed by the error bar. ZnPyP exhibits an enhanced CPD under UV light exposure when compared to its H_2PyP, although neither molecule exhibits significant CPD changes with exposure to visible light or in the dark. This reaction is brought on by the porphyrin component's peak absorption, which extends into the visible spectrum, and the intensification under UV light is caused by the pyrene component's absorption in the ultraviolet spectrum. H_2PyP and ZnPyP. However, a striking difference in the CPD value results from the presence of greater absorption in the UV and visible regions as well as the presence of strong red-shifted excimers.[23] Fig. 4c and Fig. 4d gives the 3D raster scanned images under dark, UV and visible light exposure of H_2PyP and ZnPyP respectively.

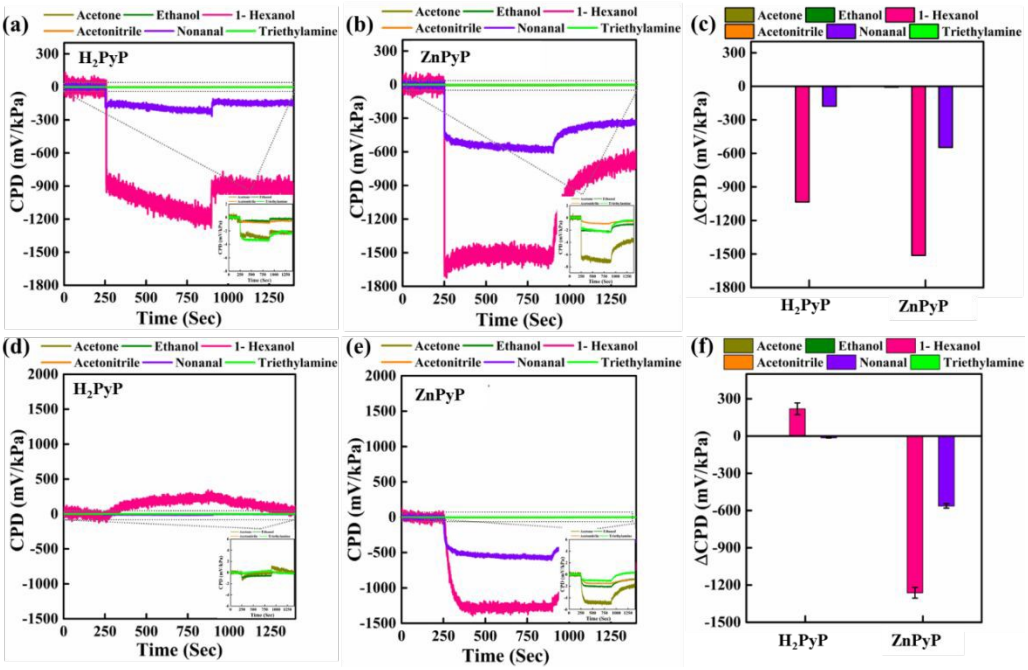

Fig. 5 Single point CPD plots under UV light illumination for H_2PyP (a), ZnPyP (b), under visible light illumination for H_2PyP(d), ZnPyP(e) with different VOCs. Change in the ΔCPD plots of H_2PyP and ZnPyP under (c) UV and (f) visible light illumination on VOCs exposure.

View Article Online
DOI: 10.1039/D4MA01228C

The switching in the CPD response upon exposure to UV radiation after maintaining the sample in dark environment under various VOCs environment is shown the Fig. 5. From the Fig. 5a and 5b, 1-hexanol demonstrated the largest photovoltage response when exposed to UV light, followed by nonanal. Upon exposure to other gases, molecules showed no significant changes in the CPD values. H_2PyP exhibited a *n-type* behaviour towards saturated vapours of 1-hexanol and nonanal, whereas an *n-type* behaviour is observed in the case of ZnPyP. Overall, the ZnPyP and H_2PyP showed better selectivity towards 1-hexanol, followed by nonanal, acetone, and ethanol as compared to the other gases. In contrary to these two gases, exposure to other gases (*viz.* acetone, ethanol, triethylamine, acetonitrile) does not produce any remarkable change in its CPD. Upon exposure to pure vapours of 1-hexanol, the H_2PyP exhibited a *n-type* behaviour as similar to ZnPyP. The behaviour of the H_2PyP in 1-hexanol environment changes as the light source is switched from a UV source to quartz tungsten halogen (QTH) as visible light source with an intensity of 70 mW/cm^2 (Fig. 5d and 5e). For both the compounds, 1-hexanol and nonanal vapours exhibits the highest levels of selectivity through the CPD change on dark to light illumination. ZnPyP showed the strongest interaction with gas molecules upon exposure to UV light. However, the ZnPyP exhibits the largest CPD shift toward 1-hexanol vapours under conditions of visible light. The donor-donor character of the molecules may be the cause of their intriguing reaction to 1-hexanol in addition to intermolecular hydrogen bonding that further supports the enhanced photo response behaviour of H_2PyP. Upon exposed to UV light, both H_2PyP and ZnPyP demonstrate as *n-type* characteristics. This phenomenon occurs as UV light excites electrons from their ground state to higher energy levels, facilitating electron transfer to the conduction band and leading to an accumulation of electrons. The accumulation of electrons results in n-type characteristics in both compounds. On the other hand, exposed to visible light H_2PyP exhibits a transition towards *p-type* characteristics. This transition can be linked to the transfer of electrons induced by light from H_2PyP to its surroundings, leading to the formation of holes within the H_2PyP framework and generating a *p-type* response. The engagement with particular VOCs, like 1-hexanol, or the intensity of the light source can additionally affect this charge transfer help to stabilize the positive charge generated on the H_2PyP. Additionally, the central Zn metal ion in ZnPyP plays a crucial role in influencing the electronic characteristics of the H_2PyP. The coordination of Zn alters the charge distribution, which may enhance the stability of the system within the *n-type* region. The maintenance of n-type characteristics in visible light, despite the presence of 1-hexanol, might be attributed to the stabilization of surplus electrons either at the Zn center or within the π-conjugated framework. In contrast, H_2PyP, which does not have metal

View Article Online
DOI: 10.1039/D4MA01228C

coordination, is lacking of the stabilizing effect provided by a central metal ion, rendering it more vulnerable to hole formation. This elucidates the transition to p-type characteristics when exposed to visible light. Consequently, the variations observed between H_2PyP and ZnPyP are mainly influenced by their charge transfer processes in response to varying light conditions, along with the stabilizing impact of Zn coordination.

The difference in CPD response on exposure to the gases under test supported by UV and visible light is depicted in Fig. 5c and 5f for H_2PyP and ZnPyP respectively. Of the six VOCs taken into consideration, 1-hexanol displayed the highest change in CPD in all modes of light. Both H_2PyP and ZnPyP show greater selectivity towards 1-hexanol exposure followed by nonanal.

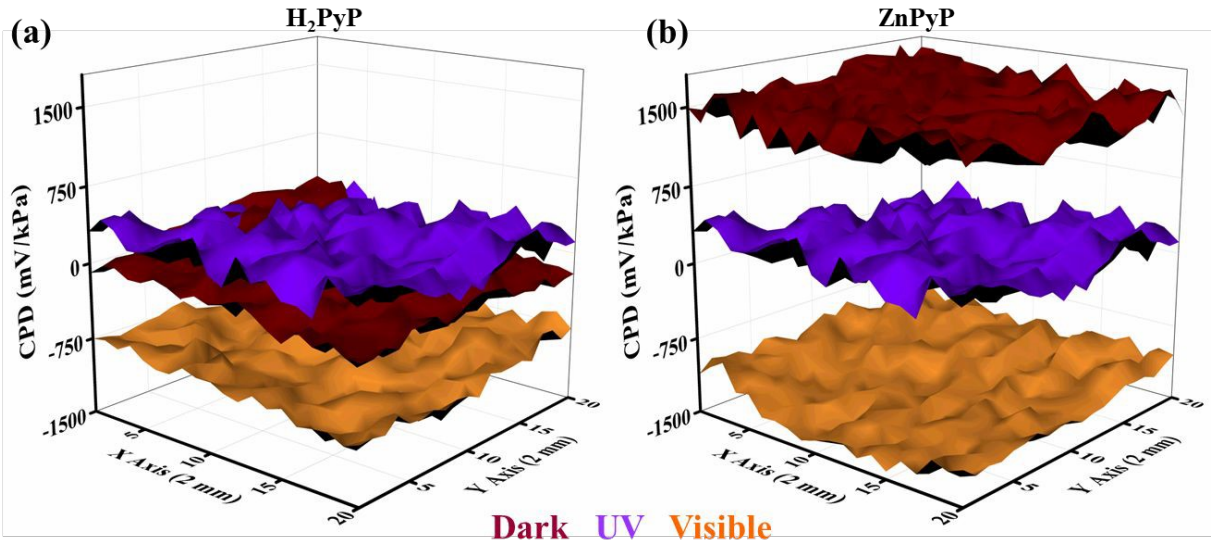

Fig. 6. 3D raster scan images in 1-hexanol of (a) H_2PyP and (b) ZnPyP in dark, UV, and visible light illumination.

Fig. 6 shows 3D raster scan images of H_2PyP and ZnPyP on FTO upon exposure to the 1-hexanol vapours to UV and visible light. The change in CPD upon exposure to UV light from dark is illustrated in Fig.6a and 6b which shows a shift in the CPD value from ~ -1500 to ~ 1500 mV/kPa. A similar shift in the CPD values towards the lower values upon exposure to light is observed in all species. In response to the interaction of H_2PyP and ZnPyP with the concerned gases, a decrease/increase in CPD occurs, which is ascertained due to strong donor (H_2PyP and ZnPyP) donor (1-hexanol) interaction that has occurred through the energy transfer process. From the literature report, PTL functionalized with MWCNTs showed under dark and light medium exhibited to show highest response in the triethylamine vapours due to the

View Article Online
DOI: 10.1039/D4MA01228C

presence of pyrene substituted with the carboxylic group at the periphery.[23] Table S2, ESI† summarizes the comparison of different porphyrins and pyrene derivatives employed for the detection of different VOCs. Fig.S11-S12 ESI† depicts the raster scan images for the interaction of H_2PyP and ZnPyP with various VOCs (ethanol, acetone, acetonitrile, triethylamine, and nonanal) in a dark and light (UV and visible) environment.

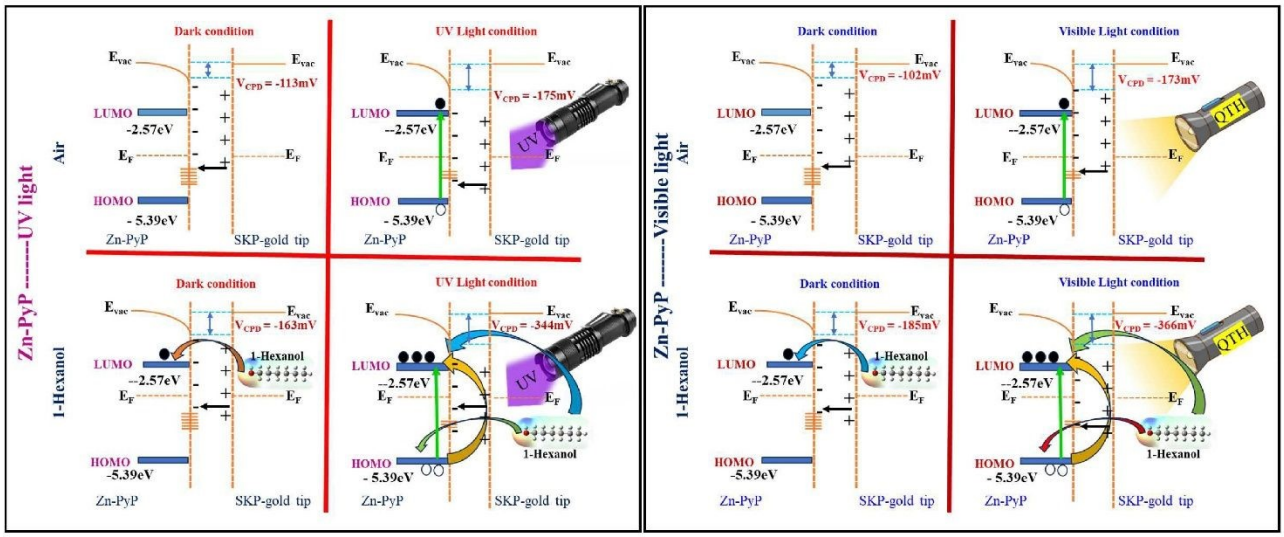

Fig. 7. Schematic illustration of energy levels of ZnPyP with reference to the gold tip of SKP instrument under dark, UV and visible light illumination conditions in ambient air and 1-hexanol media.

Fig. 7 gives the energy level diagrams of ZnPyP under UV and visible light illumination for ambient air and 1-hexanol media. Under air medium, ZnPyP exhibits a reduced CPD shift from dark to UV and visible light illumination. Due to surface states and adsorbed ionised oxygen, the dark pure ZnPyP exhibits a downward band bending under UV light conditions, with a CPD of -175 mV. Conversely, the molecule ZnPyP with a CPD of -344 mV causes downward band bending in the ZnPyP containing 1-hexanol. The photogenerated charge carriers have the ability to excite electrons from HOMO of ZnPyP to LUMO level upon involvement with UV light. However, fewer electrons are moved in this way and reach the LUMO, which lowers the electron concentration and increased the resistance. Consequently, a higher upward band is observed. On the other hand, upon exposed to 1-hexanol vapours, 1-hexanol also helps the ZnPyP LUMO by contributing electron transition from HOMO to LUMO triggered by light. Because of its weak attachment to the core carbon atom, the –OH group in 1-hexanol is easily able to give electrons to the interfering surface. As a result, there is higher downward band bending and subsequent increase in the electron concentration on the

View Article Online
DOI: 10.1039/D4MA01228C

LUMO, which lowers resistance. Under the similar conditions in dark, ZnPyP exhibits a downward band bending under visible light conditions, with a CPD of -173 mV. This is because of the surface depletion barrier brought on by surface states and adsorbed ionised oxygen. However, with a CPD of -366 mV, the ZnPyP sample containing 1-hexanol exhibits downward band bending. The photogenerated charge carriers have the ability to excite electrons from the ZnPyP HOMO level to its LUMO level upon involvement with visible light. However, fewer electrons are moved in this way and reach the LUMO, which lowers the electron concentration and increased the resistance. Consequently, a higher upward band is observed. On the other hand, when exposed to 1-hexanol vapours, 1-hexanol also helps the ZnPyP LUMO by contributing electron transition from HOMO to LUMO triggered by light. Because of its weak attachment to the core carbon atom, the –OH group in 1-hexanol is easily able to give electrons to the interfering surface. As a result, there is higher downward band bending and subsequent increase in the electron concentration on the LUMO, which lowers resistance

To ascertain the binding interaction between developed H_2PyP and ZnPyP, the DFT calculations were carried out using Gaussian16 package with hybrid exchange–correlation functional B3LYP and basis sets 6-311++G (d,p)/LANL2DZ.[39] Our previous DFT investigations have helped to understand the interaction of different VOCs with various organic molecules to validate the experimental observations.[21-23] The VOCs considered in our study are ethanol, acetone, acetonitrile, 1-hexanol, nonanal, and triethylamine (Fig. S13 ESI†). Structures of H_2PyP, ZnPyP and VOCs are modelled and optimized. For adsorption studies, a complex system containing these organic molecules and VOCs were modelled and the combined structures were optimized. The adsorption energies (E_{ads}) of the VOCs on the organic sensing molecules were calculated using the formula,

$$E_{ads} = E_{(organic\ molecule+VOC)} - E_{(organic\ molecule)} - E_{(VOC)} \qquad (3)$$

where $E_{(organic\ molecule\ +\ VOC)}$, $E_{(organic\ molecule)}$ and E_{VOC} are the total energies of the complex molecule, organic molecule and VOCs, respectively.[25] The charge transfer between the organic molecules and VOCs were calculated using Mulliken charge analysis.

The optimized structures of H_2PyP and ZnPyP along with their electrostatic potential (ESP) plots are shown in Fig. 8 and Table. 2. The red and blue regions in the ESP plot indicate the electron rich and deficient regions. From the ESP plots, it is clear that the central core is the active site for VOC interaction. So, the VOCs will interact more with the porphyrin core rather than the pyrene group, even though the pyrene group is act as an additional active site.

View Article Online
DOI: 10.1039/D4MA01228C

The HOMO-LUMO values of organic molecules and VOCs are mapped as shown in Fig. 9a. The metalation has led to a small change in the energy gap.

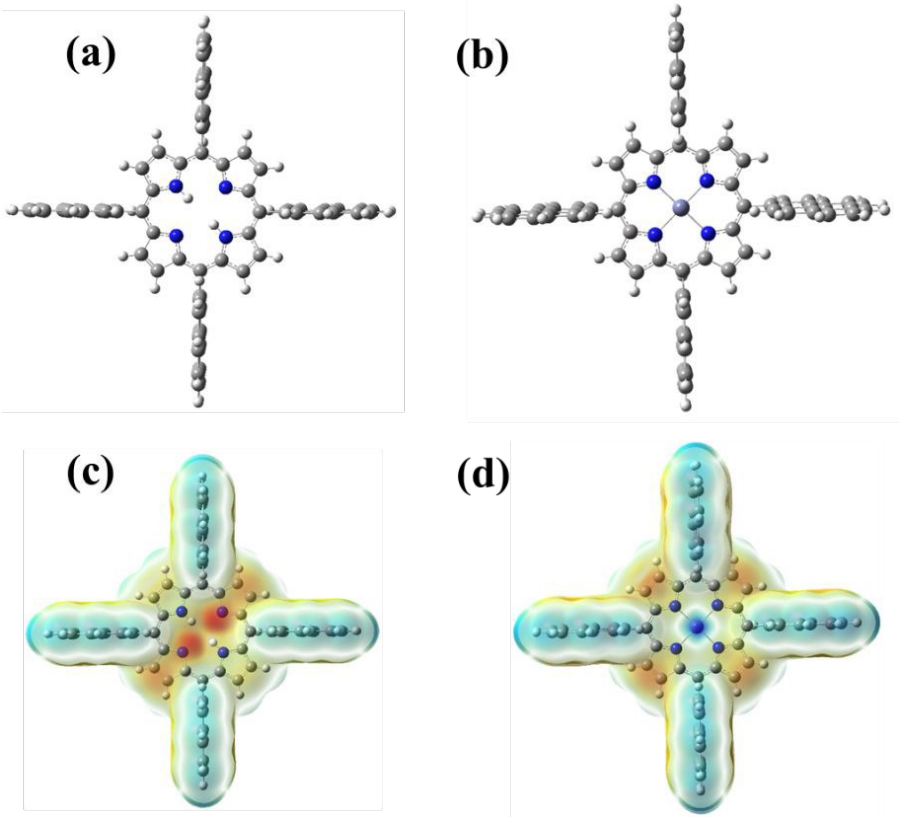

Fig. 8. Molecular structures of (a) H_2PyP, and (b) ZnPyP; ESP plot of (c) H_2PyP, and (d) ZnPyP.

Table 2. Electronic properties of organic molecules and VOCs

Molecule	HOMO (eV)	LUMO (eV)	Energy gap (eV)
H_2PyP	-5.39	-2.62	2.77
ZnPyP	-5.42	-2.56	2.86
Ethanol	-7.67	-0.36	7.31
Acetone	-7.05	-0.77	6.28
Acetonitrile	-9.26	-0.57	8.69
1-hexanol	-7.55	-0.33	7.22
Nonanal	-7.19	-0.98	6.21
Triethylamine	-5.86	-0.16	5.70

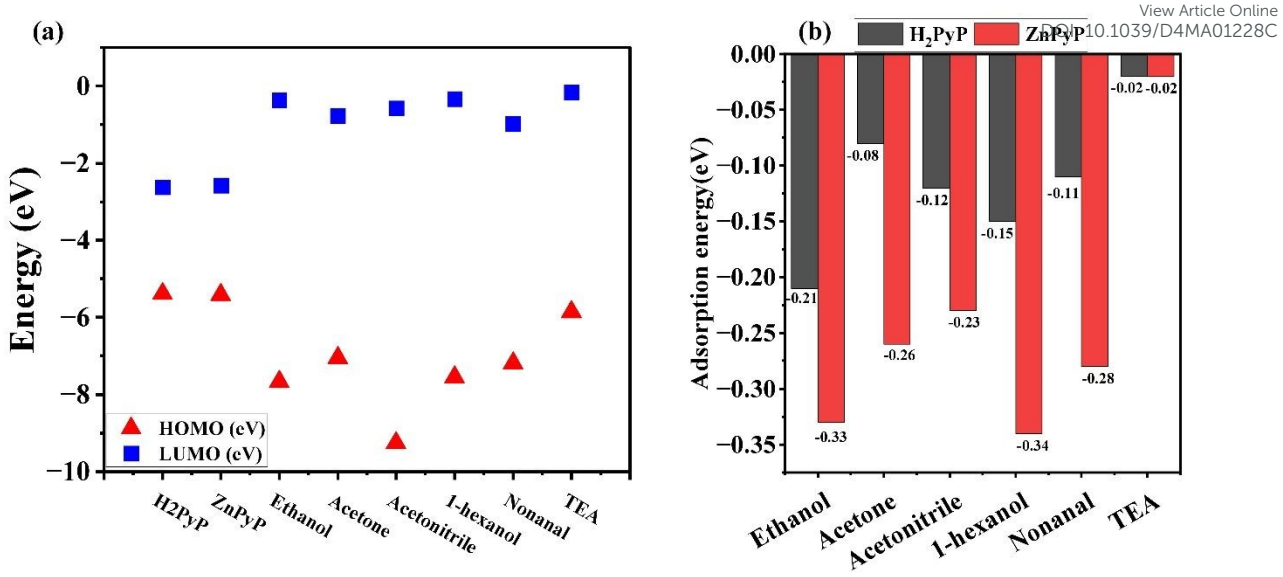

Fig. 9. (a) HOMO-LUMO values of H_2PyP, ZnPyP and VOCs (b) Adsorption energy of VOCs with H_2PyP and ZnPyP.

The VOCs are interacted with the central core as well as the peripheral ring of the organic molecules. It is found that VOCs show higher interaction with the porphyrin core. The central core site is more favourable compared to the peripheral site since higher adsorption energy was obtained at the central core site, this in agreement with the similar procedure reported on porphyrin system containing triphenylamine.[40] The adsorption energies of VOCs with all the organic molecules are represented in Fig. 9(b). The obtained energy values are in the range of -0.33 eV to -0.02 eV. As the magnitude of adsorption energy range is less than -1 eV during the interaction of VOCs with H_2PyP and ZnPyP results favourable physisorption process. However, this kind of adsorption energy range is in-line with earlier observations.[41] This confirms that all interactions are physisorption in nature. In all the cases, the VOCs are interacted more with ZnPyP than H_2PyP, so the central metal has a vital role in the adsorption. The introduction of metal improves the VOC adsorption property. Interestingly, both H_2PyP and ZnPyP molecules show higher interaction towards VOCs belonging to alcohol family particularly 1-hexanol, ethanol followed by nonanal, acetone and acetonitrile. The details on adsorption energy of VOCs with H_2PyP and ZnPyP molecules have been provided by Table S3 and S4 in ESI†. The Mulliken charge transfer between organic molecule and VOCs is shown in (Fig.S14 ESI†). A significant charge transfer has occurred between nonanal and both organic molecules. The computational results confirm that both H_2PyP and ZnPyP have more affinity towards alcohols, especially towards 1-hexanol compared to other VOCs.

4. CONCLUSIONS

View Article Online
DOI: 10.1039/D4MA01228C

In summary, we have developed freebase porphyrin and its Zn(II)complex having an orthogonal oriented pyrene units at the meso position and developed the thin films. The combined photophysical studies reveal that appreciable electronic interaction takes between the porphyrin π-system and meso-substituted pyrene units. The photophysical studies exhibited to show energy-transfer process is highly predominant with long lived charge-separated states attributed to the delocalization of the porphyrin to the pyrene units and exhibited to show as strong donor compounds. The gas adsorption studies of H_2PyP and ZnPyP with different VOCs exhibited to show good sensitivity and selectivity towards the detection of 1-hexanol vapours upon exposure to UV and visible light conditions. Under UV light condition, both H_2PyP and ZnPyP showed *n-type* behaviour while H_2PyP exhibited *p-type* and ZnPyP showed *n-type* behaviour under visible light towards 1-hexanol. H_2PyP demonstrates a significant photovoltage response of 93% within 17 seconds of exposure, accompanied by a recovery rate of 23% over 5 seconds. In contrast, ZnPyP exhibits an even higher photovoltage response of 97% in just 2 seconds, with a recovery rate of 55% achieved within 116 seconds under UV light. ZnPyP exhibits superior response and recovery time than H_2PyP due to variations in the mode of intermolecular interactions through the metal centre and efficient photoinduced energy transfer process. The surface binding studies through DFT calculations confirm the strong photoresponse of porphyrin derivatives to 1-hexanol, consistent with experimental data. Fine tuning the structure-property correlation and design strategy could be useful for developing dual-mode light-assisted chemical sensing field-effect transistors and new sensing platforms for detecting alcohols in food and the environment.

Author contributions

All authors contributed to the study. In particular: Prasanth Palanisamy: Writing–original draft, Methodology, Investigation, Formal analysis, Conceptualization. Mageshwari Anandan: Writing–original draft Methodology, Investigation, Formal analysis and Validation. Sheethal Sasi: Methodology, Investigation, Formal analysis and Validation. Arbacheena Bora: Investigation, Formal analysis and Validation. Sarath Kumar Chedharla Balaji: Investigation, Formal analysis and Validation. Rence P Reji: Investigation, Formal analysis and ValidationYoshiyuki Kawazoe: Supervision, Resources, Funding acquisition. Kommineni Kalyani: Morphology, Investigation, Formal analysis and Validation. Surya Velappa Jayaraman: Writing– review & editing, Supervision, Resources, Funding acquisition. Yuvaraj Sivalingam: Supervision, Resources, Funding acquisition. Venkatramaiah Nutalapati: Concept, Writing– review & editing, Supervision, Resources, Funding acquisition.

View Article Online
DOI: 10.1039/D4MA01228C

Data availability

The data that support the findings of this study are available from the corresponding author, upon reasonable request. Details related to the structural characterization (NMR, Mass and FT-IR), emission spectra and SKP measurements are provided in the supporting information.

Conflicts of interest

The authors declare that they have no known competing financial interests or personal relationships that could have appeared to influence the work reported in this paper.

Acknowledgments

NVR greatly acknowledges the Science & Engineering Research Board (SERB), Government of India for funding through a start-up research grant (SRG/2019/001023). Central Power Research Institute (CPRI, A government of India society under the Ministry of Power) for funding through the R&D project (CPRI/R&D/TC/GDEC/2022) and SRMIST seed grant. Y.S. and V.J.S. thank DST-SERB for the financial support under Core Research Grant (CRG/2021/006647). The authors also acknowledge the Photoluminescence spectrometer facility, NRC, and SCIF of SRMIST for analytical characterization. The authors would like to express their sincere thanks to the crew of the Center for Computational Materials Science of the Institute for Materials Research, Tohoku University, for their continuous support towards supercomputing facilities. Also, the authors thank SRM-HPCC for availing the supercomputer for computations. PP and MA thanks SRMIST for the Ph.D. fellowship.

References

1 E. David and V. C. Niculescu, *International Journal of Environmental Research and Public Health*, 2021, **18,** 13147.

2 B. P. Singh, S. S. Sohrab, M. Athar, T. A. Alandijany, S. Kumari, A. Nair, S. Kumari, K. Mehra, K. Chowdhary, S. Rahman and E. I. Azhar, *Toxics*, 2023, **11**, 165.

3 R. Epping and M. Koch, *Molecules*, 2023, **28**, 1598.

4 S. Giannoukos, B. Brkić, S. Taylor, A. Marshall and G. F. Verbeck, *Chemical Reviews*, 2016, **116**, 8146–8172.

5 M. R. Miah, M. Yang, S. Khandaker, M. M. Bashar, A. K. D. Alsukaibi, H. M. A.

Hassan, H. Znad and M. R. Awual, *Sensors and Actuators A: Physical*, 2022, **347**, 113933.

6 J. Iglesias, I. Medina, F. Bianchi, M. Careri, A. Mangia and M. Musci, *Food Chemistry*, 2009, **115**, 1473–1478.

7 R. Podduturi, G. da Silva David, R. J. da Silva, G. Hyldig, N. O. G. Jørgensen and M. Agerlin Petersen, *Food Research International*, 2023, **173**, 113375.

8 L. Makhlouf, K. El Fakhouri, S. A. Kemal, A. Aasfar, I. Meftah Kadmiri and M. El Bouhssini, *Frontiers in Horticulture*, 2024, **3**, 1–12.

9 A. Nazarov and D. Thierry, *Frontiers in Materials*, 2019, **6**, 1–17.

10 A. Schütze, T. Baur, M. Leidinger, W. Reimringer, R. Jung, T. Conrad and T. Sauerwald, *Environments - MDPI*, 2017, **4**, 1–13.

11 P. Hajivand, J. Carolus Jansen, E. Pardo, D. Armentano, T. F. Mastropietro and A. Azadmehr, *Coordination Chemistry Reviews*, 2024, **501**, 215558.

12 Y. A. Waghmare, V. N. Narwade, A. Umar, A. A. Ibrahim and M. D. Shirsat, *Chemical Physics Impact*, 2024, **8**, 100419.

13 S. Supriya, V. S. Shetti, G. Hegde, *New Journal Chem*istry 2018,**42**, 12328-12348

14 N. Nath, A. Kumar, S. Chakroborty, S. Soren, A. Barik, K. Pal and F. G. de Souza, *ACS Omega*, 2023, **8**, 4436–4452.

15 A. D. F. Dunbar, S. Brittle, T. H. Richardson, J. Hutchinson and C. A. Hunter, *Journal of Physical Chemistry B*, 2010, **114**, 11697–11702.

16 A. D. Rushi, K. P. Datta, P. Ghosh, A. Mulchandani and M. D. Shirsat, *Sensors and Actuators, B: Chemical*, 2018, **257**, 389–397.

17 R. Paolesse, S. Nardis, D. Monti, M. Stefanelli and C. Di Natale, *Chemical Reviews*, 2017, **117**, 2517–2583.

18 Z. Li, C. J. Zeman, S. Valandro, J. P. O. Bantang and K. S. Schanze, *Molecules*, 2023, **28**, 4115.

19 S. Hiroto, Y. Miyake and H. Shinokubo, *Chemical Reviews*, 2017, **117**, 2910–3043.

20 G. Magna, M. Muduganti, M. Stefanelli, Y. Sivalingam, F. Zurlo, E. Di Bartolomeo, A.

Catini, E. Martinelli, R. Paolesse and C. Di Natale, *ACS Applied Nano Materials*, 2021, **4**, 414–424.

21 G. Marappan, K. Pushparaj, Y. Sivalingam, V. Nutalapati and V. J. Surya, *Materials Letters*, 2021, **304**, 130724.

22 K. Selvaraj, G. Marappan, P. Gawas, S. Raviteja, G. Dinesh Kumar, V. Jayaraman Surya, Y. Sivalingam and V. Nutalapati, *Materials Letters*, 2021, **303**, 2–5.

23 M. Elakia, M. Gobinath, Y. Sivalingam, E. Palani, S. Ghosh, V. Nutalapati and V. J. Surya, *Physica E: Low-Dimensional Systems and Nanostructures*, 2020, **124**, 114232.

24 Y. Sivalingam, G. Magna, R. Kalidoss, S. Murugan, D. Chidambaram, V. Nutalapati, S.V. Jayaraman, R. Paolesse, C.D. Natale, *Nanotechnology*, 2022, **33**, 075503.

25 R. P. Reji, G. Marappan, Y. Sivalingam and V. Jayaraman Surya, *Materials Letters*, 2022, **306**, 130945.

26 X. Wang, S. Li, L. Zhao, C. Xu and J. Gao, *Chinese Journal of Chemical Engineering*, 2020, **28**, 532–540.

27 P. P. Gawas, A. Bora, R. P. Reji, B. Ramakrishna, P. B. Managutti, C. R. Göb, S. Mohamed, Y. Kawazoe, S. Velappa Jayaraman, Y. Sivalingam and V. Nutalapati, *Journal of Physical Chemistry C*, 2023, **127**, 6466–6482.

28 P. P. Gawas, A. Bora, R. P. Reji, S. K. Cb, B. Ramakrishna, V. Nalluri, S. V. Jayaraman, Y. Sivalingam and V. Nutalapati, *ACS Applied Electronic Materials*, 2022, **4**, 2313–2325.

29 S. Sasi, G. Marappan, Y. Sivalingam, M. Chandran, G. Magna, S. Velappa Jayaraman, R. Paolesse and C. Di Natale, *Surfaces and Interfaces*, 2024, **50**, 104456.

30 G. Marappan, A. K. Mia, K. Puspharaj, S. Vaidyanathan, Y. Kawazoe, Y. Sivalingam and V. J. Surya, *Surfaces and Interfaces*, 2024, **44**, 103648.

31 T. Zoltan, F. Vargas, C. Rivas, V. López, J. Perez and A. Biasutto, *Scientia Pharmaceutica*, 2010, **78**, 767-790.

32 T. M. Halasinski, F. Salama and L. J. Allamandola, *The Astrophysical Journal*, 2005, **628**, 555–566.

33 Y. Okabe, S. K. Lee, M. Kondo and S. Masaoka, *Journal of Biological Inorganic*

View Article Online
DOI: 10.1039/D4MA01228C

Chemistry, 2017, **22**, 713–725.

34 M. Managa, J. Britton, E.K. Amuhaya, T. Nyokong, *Journal of Luminescence*, 2017, **185**, 34-41.

35 N. S. Ramgir, P. K. Sharma, N. Datta, M. Kaur, A. K. Debnath, D. K. Aswal and S. K. Gupta, *Sensors and Actuators, B: Chemical*, 2013, **186**, 718–726.

36 Y. Sivalingam, P. Elumalai, S. V. J. Yuvaraj, G. Magna, V. J. Sowmya, R. Paolesse, K. W. Chi, Y. Kawazoe and C. Di Natale, *Journal of Photochemistry and Photobiology A: Chemistry*, 2016, **324**, 62–69.

37 Y. Sivalingam, E. Martinelli, A. Catini, G. Magna, G. Pomarico, F. Basoli, R. Paolesse and C. Di Natale, *Journal of Physical Chemistry C*, 2012, **116**, 9151–9157.

38 G. Marappan, R.P. Reji, V. Mohan, T.V.L. Kumar, Y. Sivalingam, V.J. Surya, *Journal of Materials Science: Materials in Electronics*, 2022, **33**, 9590-9598.

39 M. J. Frisch, G. W. Trucks, H. B. Schlegel, G. E. Scuseria, M. A. Robb, J. R. Cheeseman, G. Scalmani, V. Barone, G. A. Petersson, H. Nakatsuji, Gaussian 16, Gaussian. Inc., Wallingford CT 2016.

40 P. Palanisamy, M. Anandan, S. Sasi, A. Bora, R. P. Reji, C. B. S. Kumar, Y. Kawazoe, G. Raman, S. V. Jayaraman and Y. Sivalingam, *Sustainable Materials and Technologies*, 2025, e01239.

41 C. B. S. Kumar, R. P. Reji, Y. Sivalingam, Y. Kawazoe and V. J. Surya, *RSC advances*, 2024, **14**, 28182–28200.

View Article Online
DOI: 10.1039/D4MA01228C

Dr. Venkatramaiah Nutalapati
Research Assistant Professor
SRM Institute of Science & Technology
Chennai-603203
Email: nvenkat83@gmail.com

To
The Editor-in-Chief
Materials Advances

Dear Editor,

I am pleased to submit our manuscript entitled “Orthogonal effect on Pyrene-Porphyrin conjugates towards the detection of Volatile Organic Compounds under UV and Visible light illumination through Surface Photovoltage” by Prasanth Palanisamy, Mageshwari Anandan, Sheethal Sasi, Arbacheena Bora, Rence P Reji, C B Sarath Kumar, Yoshiyuki Kawazoe, K. Kalyani, Surya Velappa Jayaraman, Yuvaraj Sivalingam and myself for consideration of publication in “Materials Advances”.

All authors were agreed with the submission. This manuscript has not been published or submitted for publication elsewhere, either completely or in part, or in another form or language. We declare no competing financial interests/conflicts. The data that support the findings of this study areavailable from the corresponding author, upon reasonable request.

Thank you for your consideration.

Sincerely,

N. Venkatramaiah.

Dr. Venkatramaiah Nutalapati